Exact calculation of the minimal thickness of the large optical path difference wind imaging interferometer*

Zhang Chun-Min(张淳民)†, Ai Jing-Jing(艾晶晶), and Ren Wen-Yi(任文艺)

School of Science, Xi'an Jiaotong University, Xi'an 710049, *China*
MOE Key Laboratory for Nonequilibrium Synthesis and Modulation of Condensed Matter, Xi'an Jiaotong University, Xi'an 710049, *China*

(Received 17 May 2010; revised manuscript received 13 September 2010)

This paper gives the relation between spatial ray and its projection on paper plane based on the vector form of reflective law. Using the method of prism expansion, it obtains the exact expression of the exit height. The exit height can ensure that the incident rays, at arbitrary direction and arbitrary angle, after several transmission and reflection in the two right-angle reflectors, finally pass through the exit surface. Furthermore, it analyses the effects of different parameters on the exit height through computer simulation, and some important conclusions are obtained. The physical meaning of the sign of exit height is described, and the exact expression of the minimal thickness of the large optical path difference wind imaging interferometer is gained. This work is of great scientific significance to the static, real-time simultaneous detection of atmospheric wind field, and it will provide a theoretical and practical guidance for the miniaturization design and engineering realization of wind imaging interferometer.

Keywords: wind imaging interferometer, thickness, reflective law of vector form, prism expansion

PACS: 07.60.–j, 07.60.Rd, 42.15.Eq **DOI:** 10.1088/1674-1056/20/2/020701

1. Introduction

The passive detection principle of the upper atmospheric wind field (80 km∼300 km) is mainly based on the interference imaging spectroscopy coupled with the Doppler effect of electromagnetic wave.[1−5] We can obtain the velocity and temperature of the upper atmosphere wind field through analysing the interferogram of airglow (aurora) of atomic oxygen emission.[6−11] It was widely used in many fields such as military, national security, aerospace, environmental protection, astronomy physics, earth science etc.[6]

At present, the wind field detection instruments mostly based on Michelson interferometer are called the temporarily modulated imaging interferometers.[6] These instruments required high-quality mirror-scanning mechanisms, and the temporal resolution is limited by the maximum mechanical scanning rate.[12] Therefore they are not suitable for measurement of the fast changed spectrum and for real-time applications.[12]

In the late 1980s, another kind of interferometer without moving mirror was presented. They are divided into two kinds according to the splitter typically. One is based on birefringent crystal as splitter components;[14−20] the other is based on Sagnac interferometer as a prototype.[21,22] The optical path difference (OPD) of the wind imaging interferometer based on Sagnac interferometer as a prototype is very little. However, a large OPD (more than 4.2 cm) is required during the wind field detection.[7] In order to overcome this problem, Zhang *et al.* proposed an LOPD wind imaging interferometer (LOPDWII), and the exact calculation of the OPD of LOPDWII was presented in papers by Ruan *et al.*[13] However, there is no study regarding the thickness of LOPDWII.

In this paper, we will deduce the exact expression of the minimum thickness of the two right-angle reflectors based on the vector form of refractive law and prism expansion method under the condition that the ray always transmits in the two right-angle reflectors when it incidents arbitrarily. This work is very important to the miniaturization design and engineering realization of wind imaging interferometer, and it has wide application prospect for the static, real-time simultaneous detection of atmospheric wind field.

*Project supported by the Key Program of the National Natural Science Foundation of China (Grant No. 40537031), the National Natural Science Foundation of China (Grant No. 40875013), the National Defense Basic Scientific Research Program of China (Grant No. A1420080187), the National High Technology Research and Development Program of China (Grant No. 2006AA12Z152), and Xianyang Normal University Research Fund (Grant No. 06XSYK268).

†Corresponding author. E-mail: zcm@mail.xjtu.edu.cn

© 2011 Chinese Physical Society and IOP Publishing Ltd

2. Theoretical analysis

2.1. The relation between the spatial ray and its projection

2.1.1. The vector form of refractive and reflective law

The interface of some media is very complex in the spatial distribution, one can apply the calculation of vector form to express the propagation direction of the arbitrary ray after reflection and refraction to solve the problem. It is very convenient to describe the prism-reflection. In this paper, based on the vector form of refractive and reflective law the relation between the spatial ray and its projection is given.

The vector form of refractive law is expressed as[23]

$$\boldsymbol{A}^{0'} = (n\boldsymbol{A}^0 + \Gamma\boldsymbol{N}^0)/n', \tag{1}$$

$$\begin{aligned}\Gamma &= n'\cos i' - n\cos i \\ &= \sqrt{n'^2 - n^2 + n^2\cos^2 i} - n\cos i,\end{aligned} \tag{2}$$

where $\boldsymbol{A}^0$, $\boldsymbol{A}^{0'}$, $\boldsymbol{N}^0$ are the unit vectors of the incident ray, refractive ray and normal, respectively; n and n' are the refractive indexes of the incident and refractive space respectively.

Provided that vector is positive from left to right, otherwise negative. The normal direction is positive along the direction of ray, otherwise negative. If equations (1) and (2) take a negative value and $n = -n'$ meanwhile, they correspond to the law of reflection. The vector forms of refractive and reflective law are shown in Figs. 1(a) and 1(b), respectively.

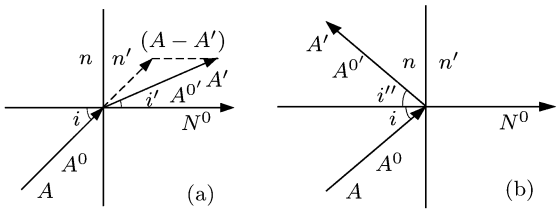


Fig. 1. Illustration of the vector form of refractive and reflective law: (a) the vector form of refractive law; (b) the vector form of reflective law.

We assume that the vectors of the incident ray, the reflective ray and the normal, respectively, are $\boldsymbol{A}^0$, $\boldsymbol{A}^{0'}$ and $\boldsymbol{N}^0$, and they are expressed as[23]

$$\begin{cases} \boldsymbol{A}_0 = x\hat{i} + y\hat{j} + z\hat{k}, \\ \boldsymbol{A}_0' = x'\hat{i} + y'\hat{j} + z'\hat{k}, \\ \boldsymbol{N}_0 = \alpha_n\hat{i} + \beta_n\hat{j} + \gamma_n\hat{k}. \end{cases} \tag{3}$$

Based on Eqs. (1)–(3), we can obtain[23]

$$\begin{pmatrix} x' \\ y' \\ z' \end{pmatrix} = \begin{pmatrix} 1-2\alpha_n^2 & -2\alpha_n\beta_n & -2\gamma_n\alpha_n \\ -2\alpha_n\beta_n & 1-2\beta_n^2 & -2\beta_n\gamma_n \\ -2\gamma_n\alpha_n & -2\beta_n\gamma_n & 1-2\gamma_n^2 \end{pmatrix} \begin{pmatrix} x \\ y \\ z \end{pmatrix}, \tag{4}$$

where x, y, z are the components of incident ray's direction along $o\hat{x}$, $o\hat{y}$, $o\hat{z}$ axes, respectively. Similarly, the direction components of reflective ray and normal are respectively (x', y', z') and $(\alpha_n, \beta_n, \gamma_n)$.

2.1.2. Relation between the spatial ray and its projection

As shown in Fig. 2, the split component of the wind imaging interferometer consists of two right-angled trapezoid reflectors, denoted by I and II, respectively. The acute angle of I and II is 45°. We assume that a and b are transverse lengths for the two right-angle reflectors, h_1 and h_2 are side lengths of them respectively, c is the dislocation between the reflectors, and $t_{\rm mt}$ is the minimal thickness of I and II.

An incident ray reaches an incoming surface denoted by MM' with an arbitrary direction, and the intersection is S. The incident angle is denoted as i, and its range is from 0 to $\pi/2$. On the boundary surface of two right-angled trapezoid reflectors, the ray SS_1 can be split up into two beams whose intensities are equal because the surface is coated with semipermeable membrane. After several transmissions and reflections in the two right-angled trapezoid reflectors, the rays have passed through the exit surface denoted by RR' finally. The propagation of the beams is shown in Fig. 2 evidently.

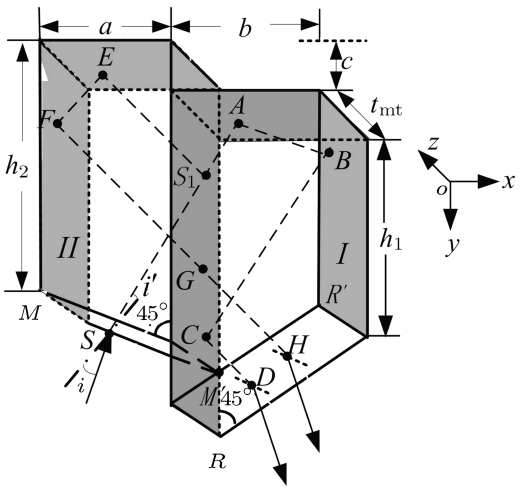


Fig. 2. Structure and optical principle of LOPDWII.

The direction vectors of the rays SA, AB, BC and CD, are denoted as $\boldsymbol{A}_1^0$, $\boldsymbol{A}_2^0$, $\boldsymbol{A}_3^0$ and $\boldsymbol{A}_4^0$, respectively; the normal direction vectors at the points S, A, B and C, are $\boldsymbol{N}_1^0$, $\boldsymbol{N}_2^0$, $\boldsymbol{N}_3^0$ and $\boldsymbol{N}_4^0$, respectively. The reference frame is defined as that $o\hat{x}$ lies along the surface of the plate, $o\hat{y}$ is the inner surface normal and $o\hat{z}$ completes the left-handed system. Thereby, the direction vectors of the refractive ray is given as

$$\begin{aligned}\boldsymbol{A}_1^0 &= x\hat{i} + y\hat{j} + z\hat{k} \\ &= \sqrt{2}(\cos i' - \sin i' \cos\theta)/2\hat{i} \\ &\quad - \sqrt{2}(\cos i' + \sin i' \cos\theta)/2\hat{j} + \sin i' \sin\theta \hat{k}, \quad (5)\end{aligned}$$

where i' is the refractive angle, θ is the angle between the incident plane and xoy plane.

The expressions of the normalized direction vectors are respectively $\boldsymbol{N}_1^0 = \frac{\sqrt{2}}{2}(\hat{i} - \hat{j})$, $\boldsymbol{N}_2^0 = \hat{j}$, $\boldsymbol{N}_3^0 = -\hat{i}$, $\boldsymbol{N}_4^0 = \hat{i}$.

According to Eqs. (3) and (4), we can obtain

$$\boldsymbol{A}_2^0 = +x\hat{i} - y\hat{j} + z\hat{k}, \quad (6)$$

$$\boldsymbol{A}_3^0 = -x\hat{i} - y\hat{j} + z\hat{k}, \quad (7)$$

$$\boldsymbol{A}_0^4 = +x\hat{i} - y\hat{j} + z\hat{k}. \quad (8)$$

Based on Eqs. (5)–(8), the angle ϕ between the ray and its projection on the paper plane can be calculated from

$$\sin\phi = z = \sin i' \sin\theta. \quad (9)$$

2.2. Specific calculation of the exit heights of out beams

According to the principle of prism expansion, the reflector I of wind imaging interferometer can be expanded along the various refractive plane, and the aperture whose radius is r will usually be located in the boundary surface of I and II, as shown in Fig. 3.

We assume that the corresponding projections of the points A, B, C, D, E, F, G, H and S_1 on the paper plane, respectively, are A_1, B_1, C_1, D_1, E_1, F_1, G_1, H_1 and S_2. The exit heights of the two out beams are denoted by t_1 and t_2.

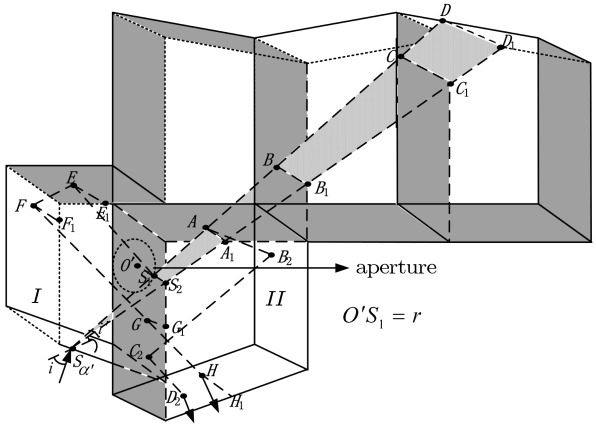


Fig. 3. Expansion graph of the right reflector.

According to Fig. 3, we can obtain

$$t_1 = DD_1 = SD_1 \mathrm{tg}\,\phi, \quad (10)$$

$$t_2 = HH_1 = SH_1 \mathrm{tg}\,\phi, \quad (11)$$

As shown in Fig. 4, SS' is perpendicular to NR, the intersection is S'. We denote the length of SS' as x. According to Fig. 4, we can obtain

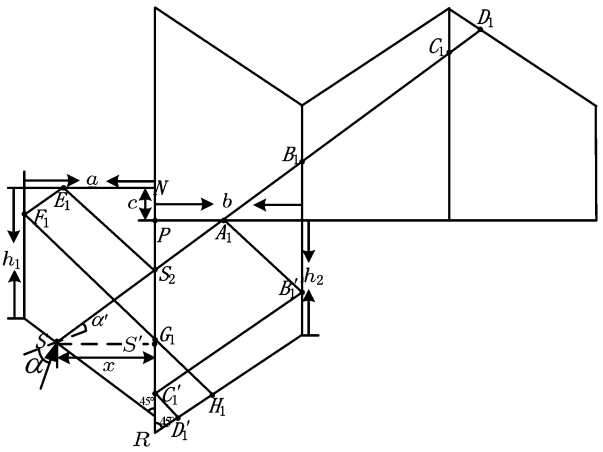


Fig. 4. Projection of the reflector II's expansion graph.

$$\begin{aligned}&SC_1 = (x + 2b)/\sin(\pi/4 - \alpha'), \\ &PS_2 = NS_2 - NP = (a + h_2 - c) - x[1 + \mathrm{tg}\,(\pi/4 + \alpha')], \\ &PA_1 = PS_2 \mathrm{tg}\,(\pi/4 - \alpha'), \quad C_1R = PR - PC_1 = b + h_1 - (2b - PA_1)\mathrm{tg}\,(\pi/4 + \alpha'). \quad (12)\end{aligned}$$

Based on sine theorem, we can obtain

$$\begin{aligned}C_1D_1 &= C_1R/\sqrt{2}\cos\alpha' = [b + h_1 - (2b - PA_1)\mathrm{tg}\,(\pi/4 + \alpha')]/\sqrt{2}\cos\alpha' \\ &= [(a + b + h_1 + h_2 - c - x) - (x + 2b)\mathrm{tg}\,(\pi/4 + \alpha')]/\sqrt{2}\cos\alpha'. \quad (13)\end{aligned}$$

By the same method, we can obtain

$$\begin{aligned} G_1H_1 &= G_1R/\sqrt{2}\cos\alpha' = [c+b+h_1-(2a-NE_1)\mathrm{tg}\,(\pi/4+\alpha')]/\sqrt{2}\cos\alpha' \\ &= [(a+b+h_1+h_2+c-x)-(x+2a)\mathrm{tg}\,(\pi/4+\alpha')]/\sqrt{2}\cos\alpha'. \end{aligned} \tag{14}$$

According to Eqs. (12)–(14), we can get

$$t_1 = (SC_1+C_1D_1)\mathrm{tg}\,\phi = |\mathrm{tg}\,\phi/\sqrt{2}\cos\alpha'|(a+3b+h_1+h_2-c), \tag{15}$$

$$t_2 = (SG_1+G_1H_1)\mathrm{tg}\,\phi = |\mathrm{tg}\,\phi/\sqrt{2}\cos\alpha'|(3a+b+h_1+h_2+c). \tag{16}$$

We assume that the two out beams have an identical exit height on the exit plane, denoted as t. If $t_1 > t_2$, based on Eqs. (15) and (16), we can obtain

$$(b-a-c) > 0. \tag{17}$$

Correspondingly, the identical exit height is expressed as

$$t = t_1 = |\mathrm{tg}\,\phi/\sqrt{2}\cos\alpha'|(a+3b+h_1+h_2-c). \tag{18}$$

If $t_1 \le t_2$, according to Eqs. (15) and (16) , we can obtain

$$(b-a-c) \le 0, \tag{19}$$

and the identical exit height is

$$t = t_2 = |\mathrm{tg}\,\phi/\sqrt{2}\cos\alpha'|(3a+b+h_1+h_2+c), \tag{20}$$

where $\mathrm{tg}\,\phi = \sin i'\sin\theta/\sqrt{1-\sin^2 i'\sin^2\theta}$, $\mathrm{tg}\,\alpha' = \mathrm{tg}\,i'\cos\theta$, $\sin i = n\sin i'$.

Based on Eqs. (18) and (20), we find that t is a function of a, b, c, h_1, h_2, i and θ.

3. Simulation and discussion

In this section, we shall make some computer simulations to verify the former theory. It can be simulated via the two parts as follows: in the first part, giving $a = 3.75$ cm, $b = 4.80$ cm, $c = 0.91$ cm, $h_1 = 5.51$ cm and $h_2 = 5.05$ cm; in the second part, giving $a = 4.80$ cm, $b = 3.75$ cm, $c = 0.91$ cm, $h_1 = 5.51$ cm and $h_2 = 5.05$ cm. The right-angled trapezoid reflectors are both made of K9 glass whose refractive index is $n = 1.5148$ at the wavelength $\lambda = 630$ nm.

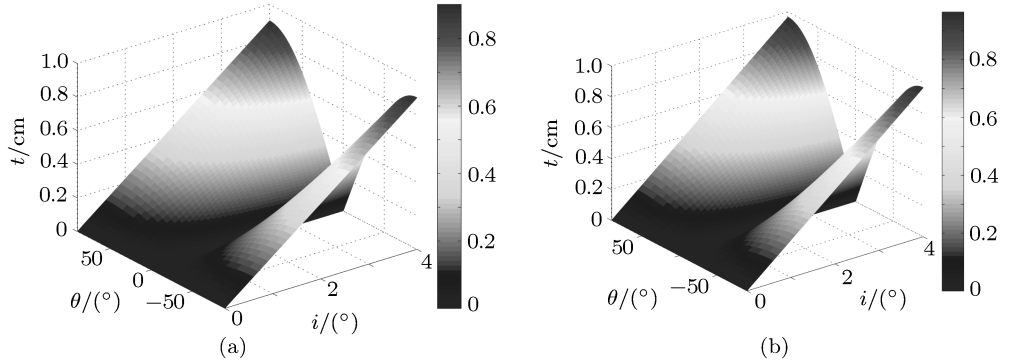


Fig. 5. The exit height t as a function of i and θ: (a) the variation surface of t with i and θ when $(b-a-c) > 0$; (b) the variation surface of t with i and θ when $(b-a-c) \le 0$.

The variation of t with i and θ is depicted as Figs. 5(a) and 5(b). During the simulation process, both i and θ are variables and the others remain constant. The useful conclusions obtained from Fig. 5 are as follows: the variation surfaces of Figs. 5(a) and 5(b) are even symmetric to the axis ($i \in [0°, 4°]$, $\theta = 0°$), that is, t is an even function of the angle θ and i; the value of t increases with the absolute values of i and θ, thereby, t will climb up to the peaks when the absolute values of i and θ both are the maximums meanwhile, that is, t is the maximum at points ($i = 4°$, $\theta = 90°$) and ($i = 4°$, $\theta = -90°$), and $t_{\max 1} = 0.9062$ cm in Fig. 5(a), $t_{\max 2} = 0.9655$ cm in Fig. 5(b). t is zero while $\theta = 0°$. The expression for the value of $t_{\max}$ is respectively

$$\begin{aligned} t_{\max} &= |\mathrm{tg}\,i'/\sqrt{2}|(a+3b-c+h_1+h_2) \quad (b-a-c>0), \\ t_{\max} &= |\mathrm{tg}\,i'/\sqrt{2}|(3a+b+c+h_1+h_2) \quad (b-a-c\le 0). \end{aligned} \tag{21}$$

We must take some considerations on the construction gage of the device during the engineering design process. According to Eqs. (18) and (20), we can obtain the conclusions: (i) t increases linearly with h_1 and h_2 under any conditions; (ii) t increases linearly with the increase of a and b without taking considerations on other parameters; (iii) t decreases with the increase of c when $b-a-c>0$, but increases with c when $b-a-c\leq 0$; (iv) The variation of t with a, b and c is more complicate under the two conditions: $b-a-c>0$ and $b-a-c\leq 0$, respectively. We will make a simulation to analyse it, and the simulation results are shown in Figs. 6(a) and 6(b). There is an intersection line at two planes under the condition $t_1=t_2$. The expression of the line can respectively be obtained from Eqs. (15) and (16),

$$b-a-c=0. \tag{22}$$

From Fig. 6(a), we can obtain the conclusions: t first decreases with the increase of c and then increases, but increases with the increase of b. When $a+c<4.8$, $t=t_1$, otherwise $t=t_2$. From Fig. 6(b), we can know that t increases with the increase of a and b under any conditions; the expression of intersection line is $b=a+0.91$; when b is in the range of $b>a+0.91$, $t=t_1$, otherwise $t=t_2$.

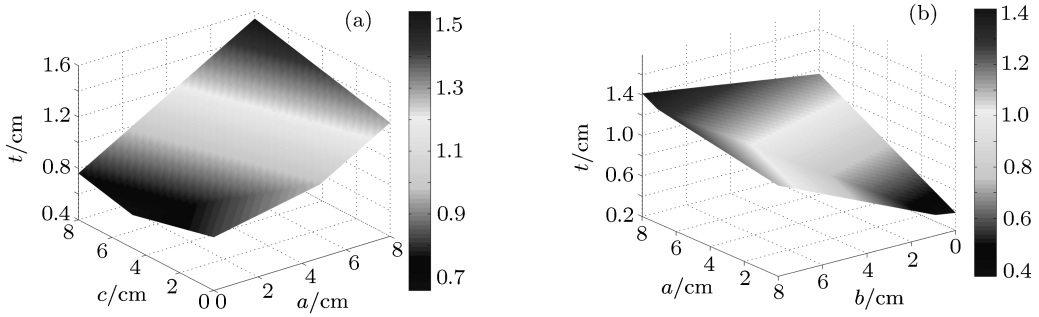


Fig. 6. The t as a function of a, b and c when $i=4°$: (a) the variation surface of t with a and c under the two conditions; (b) the variation surface of t with a and b under the two conditions.

4. The minimal thickness of LOPDWII

In fact, the propagation of refractive ray will be upward or downward when the ray incidents with an arbitrary direction, so the sign of t will be positive or negative, and the physical meaning of the sign of t can be described in Fig. 7.

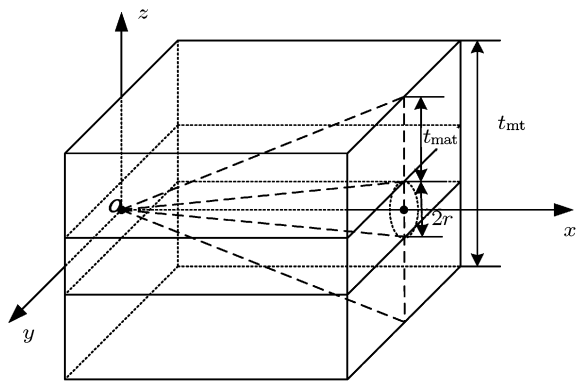


Fig. 7. The physical meaning of the sign of exit height.

Based on Fig. 7, the sign of t is identical to z axis. The expression of $t>0$ represents that the refractive ray propagates upwards, and *vice versa*. Therefore, the thickness of LOPDWII is not less than 2 times of the maximal exit height, and the minimal thickness is

$$t_{\rm mt}=2t_{\rm max}, \tag{23}$$

where $t_{\rm max}$ can be obtained from Eq. (21) while the absolute values of i and θ both are maximal. We assume that the aperture's radius which locates between the effective edge rays is denoted as r. And equation (23) is rewritten as

$$t_{\rm mt}=2(r+t_{\rm max}). \tag{24}$$

The expression of LOPDWII's OPD is[12]

$$\begin{aligned}\Delta(i,\theta)=&\sqrt{2}\{(b-a-c)n/\cos i'\\&+[(b-a)(1+\tan\alpha')+c(1-\tan\alpha')]\\&\times\sin\alpha\cos\theta/\sqrt{\sin^2\alpha'+\cos^2\alpha'\cos^2\theta}\}.\end{aligned} \tag{25}$$

Provided that $\Delta=4.2$ cm, $n=1.5148$, $i=4°$, $\theta=90°$, $b=4.80$ cm, $c=0.91$ cm, $h_1=5.51$ cm and $h_2=5.05$ cm, based on Eq. (25), we obtain the value

of a ($a = 1.93$ cm). We substitute the various parameter values into Eq. (21), according to Eq. (24), the value of LOPDWII's minimal thickness is expressed as

$$t_{\rm mt} = 2(r + 1.20) \text{ cm}.$$

5. Conclusions

The relation between the spatial ray and its projection on paper plane based on the vector form of the reflective law is given, and the exact calculation formula of the minimum thickness of LOPDWII is obtained by using the method of prism expansion. Furthermore, we have simulated the variation of the exit height t with i and θ, a and c, a and b, respectively. Through analysing and discussion, the following important conclusions are gained.

(I) The maximal exit height will be obtained at the points that the absolute values of i and θ both are maximal;

(II) Parameter t increases linearly with h_1 and h_2, a and b under any conditions;

(III) Parameter t decreases with the increase of c when $b > a + c$, but increases with the increase of c when $b \leq a + c$ without taking considerations on other parameters;

(IV) Parameter t satisfies $t = t_1$, $t = t_2$ under the conditions $b > a + c$ and $b \leq a + c$ respectively.

Furthermore, the physical meaning of the exit height corresponding to different signs is carried out, and we obtain the expression for the value of LOPDWII's minimal thickness, and it is $t_{\rm mt} = 2(r + 1.20)$ cm when $i = 4^\circ$, $\Delta = 4.2$ cm.

In the present study, a guiding theoretical foundation is established for the optical design, crystal processing, installation and debugging of LOPDWII. This work has wide application prospect for the static, real-time simultaneous detection of atmospheric wind field.

References

[1] Zhang C M, Zhao B C and Xiang L B 2000 *Acta Opt. Sin.* **20** 697 (in Chinese)

[2] Zhang C M and Jian X H 2010 *Opt. Lett.* **35** 366

[3] Zhang C M, Zhao B C, Yuan Z L and Huang W J 2009 *J. Opt.* A: *Pure Appl. Opt.* **11** 085401

[4] Zhang C M, Zhao B C and Xiang L B 2006 *Optik.* **117** 265

[5] Zhang C M, Zhao B C, Xiang L B, Li Y C and Peng Z H 2006 *Proc. SPIE* **6150** 615001

[6] Ye J Y, Zhang C M, Zhao B C and Li Y C 2008 *Acta Phys. Sin.* **57** 67 (in Chinese)

[7] Shepherd G G, Thuillier G and Gault W A, *et al.* 1993 *Geophys. Res.* **98** 10725

[8] Shepherd G G 1996 *Appl. Opt.* **35** 2764

[9] Shimoda H 2003 *Proc. SPIE* **4881** 52059

[10] Zhang C M, Zhao B C, Yuan Y and He J 2006 *Proc. SPIE* **6032** 60320T1

[11] Zhang C M and He J 2006 *Opt. Express* **14** 12561

[12] Gao Z, Xiang L B and An B Q 1998 *Opt. Technol.* **5** 33

[13] Ruan K, Zhang C M and Zhang B C 2008 *Acta Phys. Sin.* **57** 5435 (in Chinese)

[14] Zhang C M, Xiang L B and Zhao B C 2000 *Proc. SPIE* **4087** 957

[15] Zhang C M, Xiang L B and Zhao B C 2002 *Opt . Commun.* **203** 21

[16] Zhang C M, Zhao B C and Xiang L B 2003 *Opt . Commun.* **227** 221

[17] Zhang C M, Zhao B C and Xiang L B 2004 *Appl. Opt.* **43** 6090

[18] Zhang C M, Zhao B C and Xiang L B 2004 *J. Opt.* A: *Pure Appl. Opt.* **7** 613

[19] Wu L, Zhang C M and Zhao B C 2007 *Opt. Commun.* **273** 67

[20] Zhang C M, Yan X G and Zhao B C 2008 *Opt. Commun.* **281** 2050

[21] Rafert J B, Sellar R G and Blatt J H 1995 *Appl. Opt.* **34** 7228

[22] Sweedler J B and Denton M B 1989 *Appl. Spectroscopy* **43** 1378

[23] Born M and Wolf E 1999 *Principles of Optics* 7th edn. (Cambridge: Cambridge University Press) pp. 38–49